

A multispecific antibody confers pan-reactive SARS-CoV-2 neutralization and prevents immune escape

Authors:

5 John Misasi^{1#}, Ronnie R. Wei^{2#}, Lingshu Wang^{1#}, Amarendra Pegu^{1#}, Chih-Jen Wei^{2#}, Olamide
K. Oloniniyi¹, Tongqing Zhou¹, Bingchun Zhao¹, Misook Choe¹, Marika Boruszcak¹, Man
Chen¹, Kwan Leung¹, Juan Li², Eun Sung Yang¹, Zhi-Yong Yang², Yi Zhang¹, Kevin Carlton¹,
Darcy R. Harris¹, Vera B. Ivleva¹, Paula Lei¹, Cuiping Liu¹, Lindsay Longobardi¹, Adam S.
10 Olia¹, Wei Shi¹, Jeremy J. Wolff¹, Jason Gall¹, Richard A. Koup¹, Peter D. Kwong¹, John R.
Mascola¹⁺, Gary J. Nabel^{2*+}, Nancy J. Sullivan^{1*+}

Affiliations:

¹Vaccine Research Center, National Institute of Allergy and Infectious Diseases, National
Institutes of Health, Bethesda, MD 20892, USA.

15 ²Modex Therapeutics Inc., an OPKO Health Company, Natick, MA 01760, USA.

Equal contribution: #, +

*Corresponding authors: Nancy J Sullivan, Gary J. Nabel

Email: njsull@mail.nih.gov, gary.nabel@modextx.com

20 ABSTRACT

Continued evolution of the SARS-CoV-2 spike poses a challenge to immune interventions. To develop antibodies that protect against evolving SARS-CoV-2 viruses, we combined antibodies that recognize different RBD sites to generate a trivalent antibody that potently neutralized all major variants, including the most recent Omicron lineages. Negative stain electron microscopy suggests that this multispecific achieves synergistic neutralization by engaging different epitopes in specific orientations that facilitate inter-spike binding. These interactions resulted in not only improved potency but also importantly prevented virus escape, a feature not seen with parental antibody cocktails or the most potent clinical antibody. Such multispecific antibodies simplify treatment, maximize coverage, decrease the likelihood of SARS-CoV-2 escape, and provide the basis for building universal SARS-CoV-2 antibody therapies that are more likely to maintain broad reactivity for future variants.

One-Sentence Summary: SARS-CoV-2 multispecific antibodies expand neutralization breadth and potency, prevent immune escape, and simplify treatment.

35 **MAIN TEXT**

The continued viral replication and transmission of viruses during human pandemics contribute to genetic evolution that can lead to increased pathogenesis and decreased sensitivity to host immunity and antivirals. For SARS-CoV-2, variations in the spike protein have resulted in the appearance of dozens of major variants of concern (VOC). VOCs such as Beta, Delta, 40 Omicron and the newer Omicron sub-lineages contain several to dozens of amino acid variations in their spike protein that have been associated with decreased vaccine and therapeutic antibody efficacy (*1*). Among nine antibodies that have previously been, or are currently, approved as COVID-19 therapeutics (*2–16*), most have lost potency and/or breadth against evolving and variable circulating variants (**Fig 1A**). The emergence of the original Omicron (BA.1) VOC 45 resulted in high-level resistance to several therapeutic antibodies, with only COV2-2196 (tixagevimab), S309 (sotrovimab) and LY-CoV1404 (bebtelovimab) remaining active (**Fig 1A**) (*17–19*). The subsequent BA.2, BA.2.12.1 and BA.4/5 variants showed additional changes in sensitivities: COV2-2196 became inactive against to BA.4/5, REGN10987 regained activity against BA.2 and BA.2.12.1, S309 lost potency against BA.2, BA.2.12.1 and BA.4/5 and COV2- 50 2130 regained potency against BA.2, BA.2.12.1 and BA.4/5 (**Fig 1A**). This “cyclic” variation in potency is a key challenge to maintaining a portfolio of antibody-based therapies against COVID-19.

Among the clinical antibodies, only LY-CoV1404 has thus far maintained activity against all prior and current variants. However, as viral evolution continues, it is possible that resistant 55 variants will develop to any single antibody. Therefore, there is a need to identify antibody therapeutics that can maintain activity in the face of evolving viral antigenic variation. We previously identified three monoclonal antibodies (mAb), B1-182.1, A19-46.1 and A19-61.1 (hereafter termed 182.1, 46.1 and 61.1), that target distinct receptor binding domain (RBD)

epitopes and retain high potency and breadth against most VOCs (17, 20): 182.1 displays
60 subnanomolar potency against pre-Omicron VOCs (17, 20), including Beta and Delta (**Fig 1A**)
and maintains potency to BA.1, BA.1.1, BA.2 and BA.2.12.1 that is similar to mAb S309 which
showed clinical efficacy against BA.1 (21, 22); 61.1 has subnanomolar potency against Alpha,
Beta and Delta variants but loses activity to Omicron BA.1 and BA.1.1, and then recovers
neutralization activity against BA.2, BA.2.12.1 and BA.4/5 (17, 20) (**Fig 1A**); 46.1 is potently
65 neutralizing against VOC that do not contain substitutions at L452, including Beta, Gamma,
BA.1 and BA.1.1 (17, 20) (**Fig 1A**), but is inactive against BA.2.12.1 and BA.4/5 that have
L452Q or L452R. Since these antibodies target distinct epitopes and show a non-overlapping
pattern of VOC resistance, it suggested the possibility that a combination of these antibody
specificities might provide neutralization breadth against longitudinal SARS-CoV-2 variants.

70 To test this hypothesis, we combined 182.1 with either 61.1 or 46.1 as two-mAb
combinations or with both 61.1 and 46.1 as triple-mAb combination. These were tested for
neutralization activity against Beta, Delta, Omicron and Omicron sublineages and results were
compared with current clinical antibody cocktails. Consistent with previous reports, the
therapeutic cocktails, CB6 + LY-CoV555 and REGN10933 + REGN10987, are unable to
75 neutralize all VOCs (**Fig 1B**)(17, 23–25). In contrast, the combination of COV2-2196 + COV2-
2130 (e.g., tixagevimab+cilgavimab) maintained subnanomolar potency across all variants albeit
with some loss of potency (**Fig 1B**). As we previously showed (17), the combination of 182.1 +
46.1 provided synergistic neutralization against BA.1 (IC_{50} 186 pM) (**Fig 1B**) compared to the
individual components (IC_{50} 2554 and 451 pM) (**Fig 1A**). In addition, we noted similarly potent
80 synergistic neutralization against all Omicron sublineages except for BA.4/5; for which both
mAbs lack activity (**Fig 1**). The combination of 182.1 + 61.1 neutralized all variants with IC_{50}
values that were equivalent to or better than the parental antibodies (**Fig 1**), and the triple

combination of 182.1 + 61.1 + 46.1 neutralized all variants with improved overall potency compared to the double combinations (**Fig 1**). These results show that combinations of 182.1, 85 46.1 and 61.1, targeting class I, II and III sites within the SARS-CoV-2 spike RBD, respectively, achieve potent neutralization across all prior and current VOCs.

We previously developed recombinant trispecific antibodies against HIV-1 by combining arms from selected broadly neutralizing antibodies into a single molecule that showed unprecedented potency and breadth (26). These antibodies broadly neutralized >98% of 90 circulating virus strains (26) and exerted antiviral effects in non-human primates while also mitigating the generation of viral immune escape (27). We hypothesized that multispecific antibodies could be designed against SARS-CoV-2 that similarly improve breadth and neutralization reactivity to cover known and evolving antigenic variation. We utilized the cross-over of dual variable (CODV) format comprising one arm heterodimerized with two variable 95 fragment (Fv) domains and the second arm containing a single Fv domain (28). We designed nine trivalent anti-SARS-CoV-2 antibodies with bispecific (*i.e.*, two antigenic targets) or trispecific (*i.e.*, three antigenic targets) reactivity (**Fig 2A, S1, Table S1**). Five trivalent bispecific antibodies were generated: three containing two Fv182.1 (Fv182) and one Fv61.1 (Fv61) in different positions and two containing two Fv61 and one Fv182 in different positions 100 (**Fig2A, S1, Table S1**). Four trivalent trispecific antibodies containing Fv182, Fv61 and Fv46.1 (Fv46) were designed to avoid placing Fv46 and Fv61 in the same CODV arm, since they were previously shown to compete with each other (20). To confirm the activity of each Fv component within the trivalent antibodies, we used ELISA to evaluate binding to SARS-CoV-2 RBD proteins containing mutations that specifically eliminate the binding of all but one Fv; 105 specifically, these RBDs contained one or more of the previously identified knockout mutations for Fv182 (F486S), Fv46 (L452R) and Fv61 (K444E) (20) (**Fig S2B**). We found that each

component Fv within the trivalent antibodies recognized its cognate epitope as expected, with equivalent binding to the wildtype RBD where the Fv epitopes were intact (**Fig. S2C**). As a further test, we assessed the ability of each antibody to neutralize pseudoviruses with spike protein point mutations that eliminated binding of a single Fv component and showed that each trivalent multispecific mAb maintained neutralization via the remaining Fvs (**Fig S2D**). Taken together, these findings verified that the Fvs within each multispecific antibody were functioning as expected.

We next evaluated the ability of the trivalent antibodies to neutralize the SARS-CoV-2 ancestral D614G, and the Beta, Delta, BA.1, BA.1.1, BA.2, BA.2.12.1 and BA.4/5 variants. For D614G, Beta and Delta variants, all of the multispecifics neutralized with subnanomolar IC_{50} s (**Fig 2B**). Among the trivalent dual recognition (bispecific) antibodies that included 182.1 and 61.1 in different configurations, we observed that only the antibody with the 182.1/61.1-182.1 configuration maintained subnanomolar affinity against BA.1 and BA.1.1 (**Fig 2B**). These data indicate that for BA.1 and BA.1.1, the positioning of the Fv domain within a multispecific can impact neutralization potency. All of these bispecific antibodies displayed subnanomolar neutralization against BA.2 and BA.2.12.1 likely because, among the Fvs, the parental 61.1 antibody regains potent neutralization against these lineages. Interestingly, we found that having two copies of Fv61, regardless of position, significantly improved BA.4/5 neutralization >100-fold over other bispecifics antibodies containing a single Fv61 (**Fig 2B**). For the trispecific antibodies, all variants tested were neutralized with pico- to nanomolar potency. Against D614G, Beta and Delta variants IC_{50} s ranged between 30 and 364 pM (**Fig 2B**). For BA.1, BA.1.1 and BA.4/5, neutralization by 61.1/46.1-182.1 occurred with IC_{50} s of 175 pM, 274 pM and 1053 pM (**Fig 2B**), respectively, and notably for BA.1, with higher potency than the clinically effective antibody sotrovimab (IC_{50} 2074 pM) (**Fig 1A**). The 1-2 log higher potency of

61.1/46.1-182.1 for BA.1 and BA.1.1 compared to 61.1/182.1-46.1 suggests that the relative positions of 182.1 and 46.1 in the CODV arm are impacting on trispecific mAb potency. In contrast for BA.2 and BA.2.12.1, all four trispecific antibodies neutralized with IC₅₀ between 26 and 705 pM, with 61.1/46.1-182.1 again having the highest potency (**Fig 2B**). These data
135 indicate that a multispecific antibody with a precise configuration of Fv domains broadly neutralizes diverse strains (including strains that did not exist when the mAbs were made), suggesting that inter-epitope engagement increases antibody potency and breadth.

We note that the most potent and broad antibody, trispecific 61.1/46.1-182.1, contains the same component Fvs in its CODV arm as trispecific 61.1/182.1-46.1, yet neutralizes BA.1 and
140 BA.1.1 15 to 40-fold better than 61.1/182.1-46.1 (**Fig 2B**). To better understand how differences in the positions of Fv46 and Fv182 in the CODV arm of these molecules led to differences in potency, we used negative stain-electron microscopy (NSEM) to compare the binding of purified CODV 46.1-182.1 or 182.1-46.1 to D614G spike trimer proteins containing mutations that eliminate binding to either Fv46 or Fv182 (**Fig. 3A**). Consistent with the 182 mAb epitope being
145 at the distal tip of RBDs when they are in the up position, and thus more accessible for binding by Fv, the relative position of Fv182 within the CODV arm did not influence its ability to bind to the trimer (**Fig 3B, C**). However, for Fv46 we noted CODV position-dependent binding to spike trimers. In particular, when Fv46 is in the outer position (**Fig 3D, leftmost panels**), no NSEM binding classes were observed against K444E/F486S spike protein that should be recognized by
150 Fv46 but is unable to bind Fv182 (**Fig 3D, rightmost panels**). Since CODV Fv46 binding to soluble RBD was not impacted (**Fig S2C**), these results suggests that the outer position the CODV is not compatible with binding of Fv46 to RBD domains contained within trimeric spike proteins. On the other hand, when Fv46 is in the inner position (**Fig 3E, leftmost panels**), NSEM class averages show that Fv46 binds K444E/F486S spike protein (**Fig 3E, center-right**).

155 Representative models of the binding mode observed in the NSEM micrographs show that when Fv46
is in the outer position (**Fig 3E, right panel**), its angle of approach allows the CHCL1-Fv182
portions of the CODV to be positioned away from the spike trimer, thereby avoiding potential
clashes with the spike trimer. Since NSEM of CODV 46.1-182.1 revealed that both Fv domains
can bind spike trimers, we hypothesized that the CODV 46.1-182.1 alone would be sufficient to
160 cross-link Omicron spike trimers. Indeed, NSEM micrographs revealed that aggregates were
formed when CODV 46.1-182.1 was incubated with Omicron spike trimers (**Fig 3E**). Taken
together, these results illustrate how in the context of spike trimers, both the location of epitopes
within RBD and CODV position can impact binding, aggregative potential and neutralization.
Specifically, Fvs with an angle of approach vertical to the trimer apex such as Fv182 are likely to
165 have greater flexibility for positioning with trivalent mAb designs, likely due to freedom from
steric constraints, and consistent with higher potency neutralization by this Fv. In contrast, Fv46
has a lateral or angled approach suggesting that antibodies that bind with this angle of approach
may be subject to steric constraints that are revealed by position-dependence of the Fv for
optimal engagement and neutralization.

170 The perpetuation of the COVID-19 pandemic due to waves of infection by emerging
VOC has demonstrated the impact of viral evolution and in particular, the impact of antigenic
changes in the spike protein, on virus persistence. We previously showed that replication-
competent vesicular stomatitis virus (rcVSV) pseudotyped with the SARS-CoV-2 spike can
rapidly mutate to escape neutralization by the individual antibodies 182.1, 46.1 or 61.1 (20). We
175 therefore sought to compare the potential for escape from the trivalent antibody with the broadest
and most potent neutralization activity, 61.1/46.1-182.1, against the triple antibody cocktail or
the individual mAbs, 182.1 and LY-CoV1404. Under conditions where 182.1 and LY-CoV1404
fully escaped antibody neutralization (i.e., >20% cytopathic effect at 333,333 pM) within 2-3

180 rounds of repeated infection *in vitro* (**Fig 4**), we found that an equal mixture of 182.1 + 61.1 +
46.1 slowed acquisition of the escaped phenotype, but gradually lost neutralization potency
during 7 rounds of infection (**Fig 4**). For trispecific, 61.1/46.1-182.1, there was no observed
escape in two independent experiments; though from round 1 to round 2 of replication there was
a modest shift in the mAb concentration (107pM) required to maintain <20% CPE, in line with
neutralization potency determinations that would not be expected to fully suppress viral growth
185 (**Fig 2B and 4**). The ability of this trivalent mAb to mitigate neutralization escape corresponds
with the observation that the CODV arm of 61.1/46.1-182.1 can also cross-link and aggregate
spikes due to both Fv components being able to bind RBD (**Fig 3C, E and F**). Since the
individual mAbs and mAb cocktail would not be expected to crosslink spikes. These results
suggest that the potency and improved escape mitigation of 61.1/46.1-182.1 over the antibody
190 cocktail is mediated by the ability to trivalent mAbs to engage and aggregate multiple trimers.

In this report, we developed trivalent bispecific and trispecific antibodies that target
independent epitopes on the viral spike. These antibodies are highly potent and maintain breadth
against VOCs with evolving patterns of antigenic variation, including the most recent Omicron
sublineages. The combination of three antibody specificities in a precise orientation within one
195 molecule ensured that the antibody could neutralize VOC with IC_{50} s in a range similar to, or better
than, clinically active antibodies, even when only one antibody Fv domain was active. In addition,
the trispecific antibody mitigated virus escape *in vitro* under conditions where highly potent and
broad single monoclonal antibodies could not, even when combined as cocktails. While the
antibodies in this study were initially isolated prior to the emergence of Omicron, the strategy of
200 rationally choosing antibody specificities that target distinct antigenic sites on spike, and that are
differentially impacted by VOC mutations, allowed the generation of a broadly active molecule
that neutralized future variants (unforeseen at the time of CODV design). Furthermore, the

inclusion of multiple specificities on the same molecule has the potential of additive or synergistic binding and restriction of pathways for viral escape. Finally, the results in this report suggest the possibility that vaccine antigens targeting the functionally constrained epitopes contained in this trispecific antibody might increase breadth and potency against current and future variants using a single protein with simplified clinical development.

References and Notes

1. F. Wu, S. Zhao, B. Yu, Y. M. Chen, W. Wang, Z. G. Song, Y. Hu, Z. W. Tao, J. H. Tian, Y. Y. Pei, M. L. Yuan, Y. L. Zhang, F. H. Dai, Y. Liu, Q. M. Wang, J. J. Zheng, L. Xu, E. C. Holmes, Y. Z. Zhang, A new coronavirus associated with human respiratory disease in China. *Nature*. **579**, 265–269 (2020).
2. B. E. Jones, P. L. Brown-Augsburger, K. S. Corbett, K. Westendorf, J. Davies, T. P. Cujec, C. M. Wiethoff, J. L. Blackbourne, B. A. Heinz, D. Foster, R. E. Higgs, D. Balasubramaniam, L. Wang, Y. Zhang, E. S. Yang, R. Bidshahri, L. Kraft, Y. Hwang, S. Žentelis, K. R. Jepson, R. Goya, M. A. Smith, D. W. Collins, S. J. Hinshaw, S. A. Tycho, D. Pellacani, P. Xiang, K. Muthuraman, S. Sobhanifar, M. H. Piper, F. J. Triana, J. Hendle, A. Pustilnik, A. C. Adams, S. J. Berens, R. S. Baric, D. R. Martinez, R. W. Cross, T. W. Geisbert, V. Borisevich, O. Abiona, H. M. Belli, M. de Vries, A. Mohamed, M. Dittmann, M. I. Samanovic, M. J. Mulligan, J. A. Goldsmith, C.-L. Hsieh, N. V Johnson, D. Wrapp, J. S. McLellan, B. C. Barnhart, B. S. Graham, J. R. Mascola, C. L. Hansen, E. Falconer, The neutralizing antibody, LY-CoV555, protects against SARS-CoV-2 infection in non-human primates. *Sci Transl Med* (2021), doi:10.1126/scitranslmed.abf1906.
3. R. Shi, C. Shan, X. Duan, Z. Chen, P. Liu, J. Song, T. Song, X. Bi, C. Han, L. Wu, G. Gao, X. Hu, Y. Zhang, Z. Tong, W. Huang, W. J. Liu, G. Wu, B. Zhang, L. Wang, J. Qi, H. Feng, F.-S. Wang, Q. Wang, G. F. Gao, Z. Yuan, J. Yan, A human neutralizing antibody targets the receptor-binding site of SARS-CoV-2. *Nature*. **584**, 120–124 (2020).
4. J. Hansen, A. Baum, K. E. Pascal, V. Russo, S. Giordano, E. Wloga, B. O. Fulton, Y. Yan, K. Koon, K. Patel, K. M. Chung, A. Hermann, E. Ullman, J. Cruz, A. Rafique, T. Huang, J. Fairhurst, C. Libertiny, M. Malbec, W.-Y. Lee, R. Welsh, G.

- 245 Farr, S. Pennington, D. Deshpande, J. Cheng, A. Watty, P.
Bouffard, R. Babb, N. Levenkova, C. Chen, B. Zhang, A.
Romero Hernandez, K. Saotome, Y. Zhou, M. Franklin, S.
Sivapalasingam, D. C. Lye, S. Weston, J. Logue, R. Haupt, M.
Frieman, G. Chen, W. Olson, A. J. Murphy, N. Stahl, G. D.
Yancopoulos, C. A. Kyratsous, Studies in humanized mice and
convalescent humans yield a SARS-CoV-2 antibody cocktail.
Science. **369**, 1010–1014 (2020).
- 250 5. S. J. Zost, P. Gilchuk, J. B. Case, E. Binshtein, R. E. Chen, J. P.
Nkolola, A. Schäfer, J. X. Reidy, A. Trivette, R. S. Nargi, R. E.
Sutton, N. Suryadevara, D. R. Martinez, L. E. Williamson, E.
C. Chen, T. Jones, S. Day, L. Myers, A. O. Hassan, N. M.
255 Kafai, E. S. Winkler, J. M. Fox, S. Shrihari, B. K. Mueller, J.
Meiler, A. Chandrashekar, N. B. Mercado, J. J. Steinhardt, K.
Ren, Y.-M. Loo, N. L. Kallewaard, B. T. McCune, S. P. Keeler,
M. J. Holtzman, D. H. Barouch, L. E. Gralinski, R. S. Baric, L.
B. Thackray, M. S. Diamond, R. H. Carnahan, J. E. Crowe,
260 Potently neutralizing and protective human antibodies against
SARS-CoV-2. *Nature*. **584**, 443–449 (2020).
6. D. Pinto, Y. Park, M. Beltramello, A. C. Walls, M. A. Tortorici,
S. Bianchi, S. Jaconi, K. Culap, F. Zatta, A. De Marco, A.
Peter, B. Guarino, R. Spreafico, E. Cameroni, J. B. Case, R. E.
265 Chen, C. Havenar-Daughton, G. Snell, A. Telenti, H. W.
Virgin, A. Lanzavecchia, M. S. Diamond, K. Fink, D. Veessler,
D. Corti, Cross-neutralization of SARS-CoV-2 by a human
monoclonal SARS-CoV antibody. *Nature*. **583**, 290–295
(2020).
- 270 7. L. Piccoli, Y. J. Park, M. A. Tortorici, N. Czudnochowski, A.
C. Walls, M. Beltramello, C. Silacci-Fregni, D. Pinto, L. E.
Rosen, J. E. Bowen, O. J. Acton, S. Jaconi, B. Guarino, A.
Minola, F. Zatta, N. Sprugasci, J. Bassi, A. Peter, A. De Marco,
J. C. Nix, F. Mele, S. Jovic, B. F. Rodriguez, S. V. Gupta, F.
275 Jin, G. Piumatti, G. Lo Presti, A. F. Pellanda, M. Biggiogero,
M. Tarkowski, M. S. Pizzuto, E. Cameroni, C. Havenar-
Daughton, M. Smithey, D. Hong, V. Lepori, E. Albanese, A.
Ceschi, E. Bernasconi, L. Elzi, P. Ferrari, C. Garzoni, A. Riva,
G. Snell, F. Sallusto, K. Fink, H. W. Virgin, A. Lanzavecchia,
D. Corti, D. Veessler, Mapping Neutralizing and
280 Immunodominant Sites on the SARS-CoV-2 Spike Receptor-
Binding Domain by Structure-Guided High-Resolution
Serology. *Cell*. **183**, 1024-1042.e21 (2020).
- 285 8. W. Dejnirattisai, J. Huo, D. Zhou, J. Zahradnik, P. Supasa, C.
Liu, H. M. E. Duyvesteyn, H. M. Ginn, A. J. Mentzer, A.
Tuekprakhon, R. Nutalai, B. Wang, A. Dijokaite, S. Khan, O.
Avinoam, M. Bahar, D. Skelly, S. Adele, S. A. Johnson, A.
Amini, T. Ritter, C. Mason, C. Dold, D. Pan, S. Assadi, A.
Bellass, N. Omo-Dare, D. Koeckerling, A. Flaxman, D. Jenkin,
P. K. Aley, M. Voysey, S. A. Costa Clemens, F. G. Naveca, V.

- 290 Nascimento, F. Nascimento, C. Fernandes da Costa, P. C.
Resende, A. Pauvolid-Correa, M. M. Siqueira, V. Baillie, N.
Serafin, Z. Ditse, K. Da Silva, S. Madhi, M. C. Nunes, T.
Malik, P. J. M. Openshaw, J. K. Baillie, M. G. Semple, A. R.
Townsend, K.-Y. A. Huang, T. K. Tan, M. W. Carroll, P.
295 Klenerman, E. Barnes, S. J. Dunachie, B. Constantinides, H.
Webster, D. Crook, A. J. Pollard, T. Lambe, O. consortium, I.
consortium, N. G. Paterson, M. A. Williams, D. R. Hall, E. E.
Fry, J. Mongkolsapaya, J. Ren, G. Schreiber, D. I. Stuart, G. R.
Screaton, *bioRxiv*, in press, doi:10.1101/2021.12.03.471045.
- 300 9. A. J. Greaney, T. N. Starr, C. O. Barnes, Y. Weisblum, F.
Schmidt, M. Caskey, C. Gaebler, A. Cho, M. Agudelo, S.
Finkin, Z. Wang, D. Poston, F. Muecksch, T. Hatziiannou, P.
D. Bieniasz, D. F. Robbiani, M. C. Nussenzweig, P. J.
Bjorkman, J. D. Bloom, Mapping mutations to the SARS-CoV-
305 2 RBD that escape binding by different classes of antibodies.
Nature Communications. **12** (2021), doi:10.1038/s41467-021-
24435-8.
- 310 10. D. K. Ryu, B. Kang, H. Noh, S. J. Woo, M. H. Lee, P. M.
Nuijten, J. I. Kim, J. M. Seo, C. Kim, M. Kim, E. Yang, G.
Lim, S. G. Kim, S. K. Eo, J. ah Choi, M. Song, S. S. Oh, H. Y.
Chung, A. S. Tijmsa, C. A. van Baalen, K. S. Kwon, S. Y. Lee,
The in vitro and in vivo efficacy of CT-P59 against Gamma,
Delta and its associated variants of SARS-CoV-2. *Biochemical
and Biophysical Research Communications*. **578**, 91–96 (2021).
- 315 11. C. Kim, D. K. Ryu, J. Lee, Y. Il Kim, J. M. Seo, Y. G. Kim, J.
H. Jeong, M. Kim, J. I. Kim, P. Kim, J. S. Bae, E. Y. Shim, M.
S. Lee, M. S. Kim, H. Noh, G. S. Park, J. S. Park, D. Son, Y.
An, J. N. Lee, K. S. Kwon, J. Y. Lee, H. Lee, J. S. Yang, K. C.
Kim, S. S. Kim, H. M. Woo, J. W. Kim, M. S. Park, K. M. Yu,
320 S. M. Kim, E. H. Kim, S. J. Park, S. T. Jeong, C. H. Yu, Y.
Song, S. H. Gu, H. Oh, B. S. Koo, J. J. Hong, C. M. Ryu, W. B.
Park, M. don Oh, Y. K. Choi, S. Y. Lee, A therapeutic
neutralizing antibody targeting receptor binding domain of
SARS-CoV-2 spike protein. *Nature Communications*. **12**, 1–10
325 (2021).
- 330 12. D. F. Robbiani, C. Gaebler, F. Muecksch, J. C. C. Lorenzi, Z.
Wang, A. Cho, M. Agudelo, C. O. Barnes, A. Gazumyan, S.
Finkin, T. Hägglöf, T. Y. Oliveira, C. Viant, A. Hurley, H.-H.
Hoffmann, K. G. Millard, R. G. Kost, M. Cipolla, K. Gordon,
F. Bianchini, S. T. Chen, V. Ramos, R. Patel, J. Dizon, I.
Shimeliovich, P. Mendoza, H. Hartweger, L. Nogueira, M.
Pack, J. Horowitz, F. Schmidt, Y. Weisblum, E. Michailidis, A.
W. Ashbrook, E. Waltari, J. E. Pak, K. E. Huey-Tubman, N.
Koranda, P. R. Hoffman, A. P. West, C. M. Rice, T.
335 Hatziiannou, P. J. Bjorkman, P. D. Bieniasz, M. Caskey, M.
C. Nussenzweig, Convergent antibody responses to SARS-

- CoV-2 in convalescent individuals. *Nature*. **584**, 437–442 (2020).
- 340 13. C. O. Barnes, C. A. Jette, M. E. Abernathy, K.-M. A. Dam, S. R. Esswein, H. B. Gristick, A. G. Malyutin, N. G. Sharaf, K. E. Huey-Tubman, Y. E. Lee, D. F. Robbiani, M. C. Nussenzweig, A. P. West, P. J. Bjorkman, SARS-CoV-2 neutralizing antibody structures inform therapeutic strategies. *Nature*. **588**, 682–687 (2020).
- 345 14. C. G. Rappazzo, L. V. Tse, C. I. Kaku, D. Wrapp, M. Sakharkar, D. Huang, L. M. Deveau, T. J. Yockachonis, A. S. Herbert, M. B. Battles, C. M. O'Brien, M. E. Brown, J. C. Geoghegan, J. Belk, L. Peng, L. Yang, Y. Hou, T. D. Scobey, D. R. Burton, D. Nemazee, J. M. Dye, J. E. Voss, B. M. Gunn, J. S. McLellan, R. S. Baric, L. E. Gralinski, L. M. Walker, Broad and potent activity against SARS-like viruses by an engineered human monoclonal antibody. *Science*. **371**, 823–829 (2021).
- 350 15. K. Westendorf, S. Žentelis, D. Foster, P. Vaillancourt, M. Wiggin, E. Lovett, J. Hendle, A. Pustilnik, J. M. Sauder, L. Kraft, Y. Hwang, R. W. Siegel, J. Chen, B. A. Heinz, R. E. Higgs, N. Kalleward, R. Goya, M. A. Smith, D. W. Collins, D. Pellacani, P. Xiang, V. De Puyraimond, M. Ricicova, L. Devorkin, C. Pritchard, O. Neill, C. Cohen, J. Dye, K. I. Huie, C. V Badger, J. Audet, J. J. Freitas, S. Hassanali, I. Hughes, H. C. Palma, B. Ramamurthy, R. W. Cross, T. W. Geisbert, I. Lanz, L. Anderson, P. Sipahimalani, K. S. Corbett, L. Wang, S. Yang, Y. Zhang, W. Shi, B. S. Graham, J. R. Mascola, T. L. Fernandez, C. L. Hansen, E. Falconer, B. E. Jones, B. C. Barnhart, LY-CoV1404 potently neutralizes SARS-CoV-2 variants (2021).
- 355 360 365 370 375 380 16. M. A. Tortorici, M. Beltramello, F. A. Lempp, D. Pinto, H. V. Dang, L. E. Rosen, M. McCallum, J. Bowen, A. Minola, S. Jaconi, F. Zatta, A. De Marco, B. Guarino, S. Bianchi, E. J. Lauron, H. Tucker, J. Zhou, A. Peter, C. Havenar-Daughton, J. A. Wojcechowskyj, J. B. Case, R. E. Chen, H. Kaiser, M. Montiel-Ruiz, M. Meury, N. Czudnochowski, R. Spreafico, J. Dillen, C. Ng, N. Sprugasci, K. Culap, F. Benigni, R. Abdelnabi, S.-Y. C. Foo, M. A. Schmid, E. Cameroni, A. Riva, A. Gabrieli, M. Galli, M. S. Pizzuto, J. Neyts, M. S. Diamond, H. W. Virgin, G. Snell, D. Corti, K. Fink, D. Veessler, Ultrapotent human antibodies protect against SARS-CoV-2 challenge via multiple mechanisms. *Science*. **370**, 950–957 (2020).
17. T. Zhou, L. Wang, J. Misasi, A. Pegu, Y. Zhang, D. R. Harris, A. S. Olia, C. A. Talana, E. S. Yang, M. Chen, M. Choe, W. Shi, I. T. Teng, A. Creanga, C. Jenkins, K. Leung, T. Liu, E. S. D. Stancofski, T. Stephens, B. Zhang, Y. Tsybovsky, B. S. Graham, J. R. Mascola, N. J. Sullivan, P. D. Kwong, Structural

- 385 basis for potent antibody neutralization of SARS-CoV-2
variants including B.1.1.529. *Science* (1979). **376** (2022),
doi:10.1126/science.abn8897.
- 390 18. Y. Cao, A. Yisimayi, F. Jian, W. Song, T. Xiao, L. Wang, S.
Du, J. Wang, Q. Li, X. Chen, Y. Yu, P. Wang, Z. Zhang, P.
Liu, R. An, X. Hao, Y. Wang, J. Wang, R. Feng, H. Sun, L.
Zhao, W. Zhang, D. Zhao, J. Zheng, L. Yu, C. Li, N. Zhang, R.
Wang, X. Niu, S. Yang, X. Song, Y. Chai, Y. Hu, Y. Shi, L.
Zheng, Z. Li, Q. Gu, F. Shao, W. Huang, R. Jin, Z. Shen, Y.
Wang, X. Wang, J. Xiao, X. S. Xie, BA.2.12.1, BA.4 and BA.5
395 escape antibodies elicited by Omicron infection. *Nature* (2022),
doi:10.1038/s41586-022-04980-y.
- 400 19. S. Iketani, L. Liu, Y. Guo, L. Liu, J. F. W. Chan, Y. Huang, M.
Wang, Y. Luo, J. Yu, H. Chu, K. K. H. Chik, T. T. T. Yuen, M.
T. Yin, M. E. Sobieszczyk, Y. Huang, K. Y. Yuen, H. H.
Wang, Z. Sheng, D. D. Ho, Antibody evasion properties of
SARS-CoV-2 Omicron sublineages. *Nature*. **604**, 553–556
(2022).
- 405 20. L. Wang, T. Zhou, Y. Zhang, E. S. Yang, C. A. Schramm, W.
Shi, A. Pegu, O. K. Oloniniyi, A. R. Henry, S. Darko, S. R.
Narpala, C. Hatcher, D. R. Martinez, Y. Tsybovsky, E. Phung,
O. M. Abiona, A. Antia, E. M. Cale, L. A. Chang, M. Choe, K.
S. Corbett, R. L. Davis, A. T. DiPiazza, I. J. Gordon, S. H. Hait,
T. Hermanus, P. Kgagudi, F. Laboune, K. Leung, T. Liu, R. D.
Mason, A. F. Nazzari, L. Novik, S. O’Connell, S. O’Dell, A. S.
410 O’lia, S. D. Schmidt, T. Stephens, C. D. Stringham, C. A.
Talana, I. T. Teng, D. A. Wagner, A. T. Widge, B. Zhang, M.
Roederer, J. E. Ledgerwood, T. J. Ruckwardt, M. R. Gaudinski,
P. L. Moore, N. A. Doria-Rose, R. S. Baric, B. S. Graham, A.
B. McDermott, D. C. Douek, P. D. Kwong, J. R. Mascola, N. J.
Sullivan, J. Misasi, Ultrapotent antibodies against diverse and
415 highly transmissible SARS-CoV-2 variants. *Science* (1979).
373, 0–15 (2021).
- 420 21. L. A. VanBlargan, J. M. Errico, P. J. Halfmann, S. J. Zost, J. E.
Crowe, L. A. Purcell, Y. Kawaoka, D. Corti, D. H. Fremont, M.
S. Diamond, *Nat Med*, in press, doi:10.1038/s41591-021-
01678-y.
- 425 22. D. J. Sheward, C. Kim, R. A. Ehling, A. Pankow, X. Castro
Dopico, R. Dyrdak, D. P. Martin, S. T. Reddy, J. Dillner, G. B.
Karlsson Hedestam, J. Albert, B. Murrell, Neutralisation
sensitivity of the SARS-CoV-2 omicron (B.1.1.529) variant: a
cross-sectional study. *The Lancet Infectious Diseases*. **22**, 813–
820 (2022).
- 430 23. C. K. Wibmer, F. Ayres, T. Hermanus, M. Madzivhandila, P.
Kgagudi, B. Oosthuysen, B. E. Lambson, T. de Oliveira, M.
Vermeulen, K. van der Berg, T. Rossouw, M. Boswell, V.
Ueckermann, S. Meiring, A. von Gottberg, C. Cohen, L.
Morris, J. N. Bhiman, P. L. Moore, SARS-CoV-2 501Y.V2

- escapes neutralization by South African COVID-19 donor plasma. *Nat Med.* **27**, 622–625 (2021).
- 435 24. P. Wang, M. S. Nair, L. Liu, S. Iketani, Y. Luo, Y. Guo, M. Wang, J. Yu, B. Zhang, P. D. Kwong, B. S. Graham, J. R. Mascola, J. Y. Chang, M. T. Yin, M. Sobieszczyk, C. A. Kyratsous, L. Shapiro, Z. Sheng, Y. Huang, D. D. Ho, Antibody resistance of SARS-CoV-2 variants B.1.351 and B.1.1.7. *Nature.* **593**, 130–135 (2021).
- 440 25. A. Baum, B. O. Fulton, E. Wloga, R. Copin, K. E. Pascal, V. Russo, S. Giordano, K. Lanza, N. Negron, M. Ni, Y. Wei, G. S. Atwal, A. J. Murphy, N. Stahl, G. D. Yancopoulos, C. A. Kyratsous, Antibody cocktail to SARS-CoV-2 spike protein prevents rapid mutational escape seen with individual antibodies. *Science.* **369**, 1014–1018 (2020).
- 445 26. L. Xu, A. Pegu, E. Rao, N. Doria-Rose, J. Beninga, K. McKee, D. M. Lord, R. R. Wei, G. Deng, M. Louder, S. D. Schmidt, Z. Mankoff, L. Wu, M. Asokan, C. Beil, C. Lange, W. D. Leuschner, J. Kruip, R. Sendak, Y. Do Kwon, T. Zhou, X. Chen, R. T. Bailer, K. Wang, M. Choe, L. J. Tartaglia, D. H. Barouch, S. O’Dell, J.-P. Todd, D. R. Burton, M. Roederer, M. Connors, R. A. Koup, P. D. Kwong, Z. Yang, J. R. Mascola, G. J. Nabel, Trispecific broadly neutralizing HIV antibodies mediate potent SHIV protection in macaques. *Science (1979).* **8630**, eaan8630 (2017).
- 450 27. A. Pegu, L. Xu, M. E. DeMouth, G. Fabozzi, K. March, C. G. Almasri, M. D. Cully, K. Wang, E. S. Yang, J. Dias, C. M. Fennessey, J. Hataye, R. R. Wei, E. Rao, J. P. Casazza, W. Promsote, M. Asokan, K. McKee, S. D. Schmidt, X. Chen, C. Liu, W. Shi, H. Geng, K. E. Foulds, S. F. Kao, A. Noe, H. Li, G. M. Shaw, T. Zhou, C. Petrovas, J. P. Todd, B. F. Keele, J. D. Lifson, N. A. Doria-Rose, R. A. Koup, Z. yong Yang, G. J. Nabel, J. R. Mascola, Potent anti-viral activity of a trispecific HIV neutralizing antibody in SHIV-infected monkeys. *Cell Reports.* **38**, 110199 (2022).
- 455 28. A. Ninsonoff, M. M. Rivers, Recombination of a mixture of univalent antibody fragments of different specificity. *Arch Biochem Biophys.* **93**, 460–2 (1961).
- 460 29. A. Steinmetz, F. Vallée, C. Beil, C. Lange, N. Baurin, J. Beninga, C. Capdevila, C. Corvey, A. Dupuy, P. Ferrari, A. Rak, P. Wonerow, J. Kruip, V. Mikol, E. Rao, CODV-Ig, a universal bispecific tetraivalent and multifunctional immunoglobulin format for medical applications. *MAbs.* **8**, 867–878 (2016).
- 465 30. A. M. Merchant, Z. Zhu, J. Q. Yuan, A. Goddard, C. W. Adams, L. G. Presta, P. Carter, An efficient route to human bispecific IgG. *Nature Biotechnology.* **16**, 677–681 (1998).
- 470 31. J. Zalevsky, A. K. Chamberlain, H. M. Horton, S. Karki, I. W. L. Leung, T. J. Sproule, G. A. Lazar, D. C. Roopenian, J. R.
- 475
- 480

- Desjarlais, Enhanced antibody half-life improves in vivo activity. *Nature Biotechnology*. **28**, 157–159 (2010).
- 485 32. D. H. Barouch, Z. Yang, W. Kong, B. Koriath-Schmitz, S. M. Sumida, D. M. Truitt, M. G. Kishko, J. C. Arthur, A. Miura, J. R. Mascola, N. L. Letvin, G. J. Nabel, A Human T-Cell Leukemia Virus Type 1 Regulatory Element Enhances the Immunogenicity of Human Immunodeficiency Virus Type 1 DNA Vaccines in Mice and Nonhuman Primates. *Journal of Virology*. **79**, 8828–8834 (2005).
- 490 33. A. T. Catanzaro, M. Roederer, R. A. Koup, R. T. Bailer, M. E. Enama, M. C. Nason, J. E. Martin, S. Rucker, C. A. Andrews, P. L. Gomez, J. R. Mascola, G. J. Nabel, B. S. Graham, VRC 007 Study Team, Phase I clinical evaluation of a six-plasmid multiclade HIV-1 DNA candidate vaccine. *Vaccine*. **25**, 4085–92 (2007).
- 495 34. N. A. Doria-Rose, X. Shen, S. D. Schmidt, S. O’Dell, C. McDanal, W. Feng, J. Tong, A. Eaton, M. Maglinao, H. Tang, K. E. Manning, V.-V. Edara, L. Lai, M. Ellis, K. Moore, K. Floyd, S. L. Foster, R. L. Atmar, K. E. Lyke, T. Zhou, L. Wang, Y. Zhang, M. R. Gaudinski, W. P. Black, I. Gordon, M. Guech, J. E. Ledgerwood, J. N. Misasi, A. Widge, P. C. Roberts, J. Beigel, B. Korber, R. Pajon, J. R. Mascola, M. S. Suthar, D. C. Montefiori, *medRxiv*, in press, doi:10.1101/2021.12.15.21267805.
- 500 35. L. Naldini, U. Blomer, F. H. Gage, D. Trono, I. M. Verma, Efficient transfer, integration, and sustained long-term expression of the transgene in adult rat brains injected with a lentiviral vector. *Proc Natl Acad Sci U S A*. **93**, 11382–11388 (1996).
- 505 36. Z. Y. Yang, H. C. Werner, W. P. Kong, K. Leung, E. Traggiai, A. Lanzavecchia, G. J. Nabel, Evasion of antibody neutralization in emerging severe acute respiratory syndrome coronaviruses. *Proc Natl Acad Sci U S A*. **102**, 797–801 (2005).
- 510 37. M. E. Dieterle, D. Haslwanter, R. H. Bortz, A. S. Wirchnianski, G. Lasso, O. Vergnolle, S. A. Abbasi, J. M. Fels, E. Laudermilch, C. Florez, A. Mengotto, D. Kimmel, R. J. Malonis, G. Georgiev, J. Quiroz, J. Barnhill, L.-A. Pirofski, J. P. Daily, J. M. Dye, J. R. Lai, A. S. Herbert, K. Chandran, R. K. Jangra, A Replication-Competent Vesicular Stomatitis Virus for Studies of SARS-CoV-2 Spike-Mediated Cell Entry and Its Inhibition. *Cell Host Microbe*. **28**, 486-496.e6 (2020).
- 515 38. C. Hsieh, J. A. Goldsmith, J. M. Schaub, A. M. DiVenere, H. Kuo, K. Javanmardi, K. C. Le, D. Wrapp, A. G. Lee, Y. Liu, C. Chou, P. O. Byrne, C. K. Hjorth, N. v Johnson, J. Ludes-Meyers, A. W. Nguyen, J. Park, N. Wang, D. Amengor, J. J. Lavinder, G. C. Ippolito, J. A. Maynard, I. J. Finkelstein, J. S. McLellan, Structure-based design of prefusion-stabilized SARS-CoV-2 spikes. *Science*. **369**, 1501–1505 (2020).
- 520 525

- 530 39. T. Zhou, I.-T. Teng, A. S. Olia, G. Cerutti, J. Gorman, A.
Nazzari, W. Shi, Y. Tsybovsky, L. Wang, S. Wang, B. Zhang,
Y. Zhang, P. S. Katsamba, Y. Petrova, B. B. Banach, A. S.
Fahad, L. Liu, S. N. Lopez Acevedo, B. Madan, M. Oliveira de
535 Souza, X. Pan, P. Wang, J. R. Wolfe, M. Yin, D. D. Ho, E.
Phung, A. DiPiazza, L. A. Chang, O. M. Abiona, K. S. Corbett,
B. J. DeKosky, B. S. Graham, J. R. Mascola, J. Misasi, T.
Ruckwardt, N. J. Sullivan, L. Shapiro, P. D. Kwong, Structure-
Based Design with Tag-Based Purification and In-Process
Biotinylation Enable Streamlined Development of SARS-CoV-
540 2 Spike Molecular Probes. *Cell Rep.* **33**, 108322 (2020).

Acknowledgments: We wish to acknowledge Barney Graham, for insightful discussions, and Yilie Li and Melissa Resto for insightful discussions on antibody quality control assays.

545 **Funding:** This work was funded by the Intramural Research Program of the Vaccine Research Center, NIAID, NIH and by ModeX Therapeutics, Inc.

Author contributions: J.M., L.W., A.P., R.R.W., C-J.W., Z-y.Y., T.Z. and J.L. designed experiments and analyzed data. J.M., A.P., L.W., T.Z., M.C., B.Z. O.K.O., M.B., Y.Z., E.S.Y., M.C., K.L., J.J.W., V.B.I., P.L., R.W., C.J.W., Z-y.Y. and J.L. performed experiments. W.S., A.S.O., D.R.H., M.C. and C.L. produced proteins, antibodies and other reagents. J.M., K.C., R.A.K., J.G., J.R.M, P.D.K., G.J.N. and N.J.S supervised experiments. J.M., P.D.K., J.R.M., G.J.N. and N.J.S. wrote the manuscript with help from all authors.

555 **Competing interests:** T.Z., L.W., J.M., A.P., Y.Z., E.S.Y., W.S., J.R.M, N.J.S., and P.D.K. are inventors on US patent application No. 63/147,419. R.R.W., Z-y.Y. and G.J.N are inventors on patent WO2017180913A. J.L., G.J.N., C-J.W., R.R.W., Z-y. Y. are employees of ModeX Therapeutics Inc., an OPKO Health Company. G.J.N., C-J.W, R.R.W. and Z-Y. Y. are inventors on US patent application Nos. 63/357,336 and 63/357,873. J.M., A.P., L.W., T.Z., M.C., O.K.O., B.Z., Y.Z., E.S.Y., M.C, K.L., W.S., N.J.S., J.R.M., P.D.K. and R.A.K. are inventors on the
560 same application.

Data and materials availability: All data is available in the main text or the supplementary materials.

565

Supplementary Materials

Materials and Methods

Figs. S1 to S2

Tables S1

570

A Neutralization of single candidate and clinical monoclonal antibodies against SARS-CoV-2 variants

Antibody	Generic name	Class	D614G		Beta		Delta		Omicron		Omicron Sublineages							
			IC ₅₀	IC ₈₀	B.1.351		B.1.617.2		BA.1		BA.1.1		BA.2		BA.2.12.1		BA.4/5	
					IC ₅₀	IC ₈₀	IC ₅₀	IC ₈₀	IC ₅₀	IC ₈₀	IC ₅₀	IC ₈₀	IC ₅₀	IC ₈₀	IC ₅₀	IC ₈₀	IC ₅₀	IC ₈₀
B1-182.1	--	I	10.0	39.5	30.9	107	10.0	46.2	2554	6469	1359	8267	2035	7720	1054	8762	>67,000	>67,000
COV2-2196	tixagevimab *	I	9.8	23.8	53.7	149	6.8	16.7	1722	11554	1045	5058	8077	35018	3471	36042	>67,000	>67,000
CB6	etesevimab	I	155	576	>67,000	>67,000	67.7	185	>67,000	>67,000	>67,000	>67,000	>67,000	>67,000	>67,000	>67,000	>67,000	>67,000
REGN10933	casirivimab	I	35.1	70.3	1169	6867	36.7	113	>67,000	>67,000	>67,000	>67,000	>67,000	>67,000	>67,000	>67,000	>67,000	>67,000
CT-P59	regdanvimab	I	18.8	42.3	647	2375	110	339	>67,000	>67,000	>67,000	>67,000	>67,000	>67,000	>67,000	>67,000	>67,000	>67,000
A19-46.1	--	II	86.3	244	391	1476	>67,000	>67,000	451	1523	872	2350	614	1352	>67,000	>67,000	>67,000	>67,000
LY-COV555	Bamlanivimab	II	18.9	121	>67,000	>67,000	>67,000	>67,000	>67,000	>67,000	>67,000	>67,000	>67,000	>67,000	>67,000	>67,000	>67,000	>67,000
A19-61.1	--	III	52.8	125	108	118	159	294	>67,000	>67,000	>67,000	>67,000	64.0	162	161	441	193	418
REGN10987	imdevimab	III	71.8	374	147	530	438	2015	>67,000	>67,000	>67,000	>67,000	4031	9867	3747	13924	39256	>67,000
COV2-2130	cilgavimab *	III	30.8	79.7	33.0	116	208	500	27695	>67,000	>67,000	>67,000	36.7	113	45.9	302	316	2130
S309	sotrovimab *	III	564	2017	356	2011	1044	2585	2074	8831	1390	9962	14907	>67,000	24359	>67,000	10232	63339
LY-CoV1404	bebtelovimab	III	21.7	43.7	51.4	106	70.2	131	32.7	102	18.1	44.9	8.9	21.3	10.0	37.4	7.0	24.3

pM
<10
10-100
100-1000
1000-10,000
10,000-67,000
>67,000

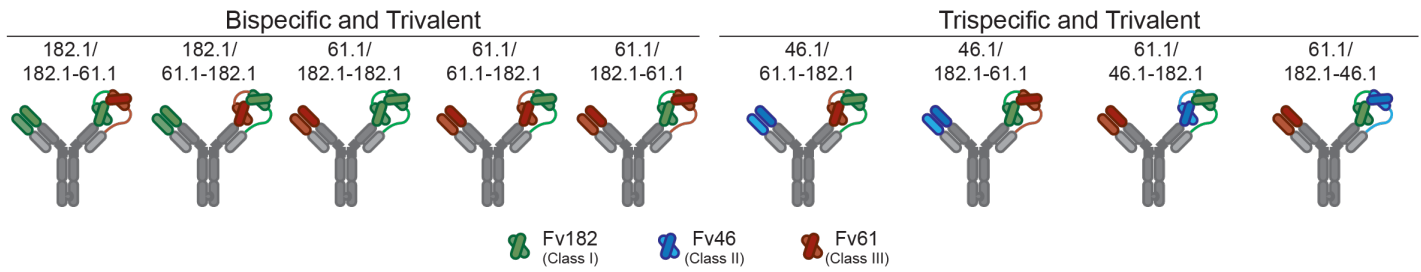
B Neutralization of monoclonal antibody combinations against SARS-CoV-2 variants

	Class	D614G		Beta		Delta		Omicron		Omicron Sublineages							
		IC ₅₀	IC ₈₀	B.1.351		B.1.617.2		BA.1		BA.1.1		BA.2		BA.2.12.1		BA.4/5	
				IC ₅₀	IC ₈₀	IC ₅₀	IC ₈₀	IC ₅₀	IC ₈₀	IC ₅₀	IC ₈₀	IC ₅₀	IC ₈₀	IC ₅₀	IC ₈₀	IC ₅₀	IC ₈₀
CB6 + LY-CoV555	I + II	37.3	94.0	>67,000	>67,000	93.1	196	>67,000	>67,000	>67,000	>67,000	>67,000	>67,000	>67,000	>67,000	>67,000	>67,000
REGN10933 + REGN10987	I + III	22.7	42.0	129	317	93.0	164	>67,000	>67,000	>67,000	>67,000	2555	5871	2434	5498	9795	16782
COV2-2196 + COV2-2130	I + III	14.7	27.3	28.7	58.7	16.0	31.8	339	911	426	1286	49.0	129	42.5	209	314	1044
B1-182.1 + A19-46.1	I + II	9.6	16.9	16.4	31.2	13.4	25.3	186	351	376	707	280	475	1454	6236	>67,000	>67,000
B1-182.1 + A19-61.1	I + III	7.5	21.2	16.2	34.9	12.6	23.4	1367	3648	1383	9832	27.0	81.7	118	274	41.3	255
B1-182.1 + A19-46.1 + A19-61.1	I + II + III	8.5	18.3	19.4	42.4	19.0	38.4	298	488	356	664	27.1	70.0	148	435	111	343

pM
<10
10-100
100-1000
1000-10,000
10,000-67,000
>67,000

Figure 1. Neutralization of SARS-CoV-2 variants by monoclonal antibodies and antibody cocktails. Neutralization of candidate and expanded access monoclonal antibodies (A) and cocktails (B) against D614G and the indicated SARS-CoV-2 variants: Beta (B.1.351), Delta (B.1.617.2), Omicron (B.1.1.529 or BA.1) and Omicron sub-lineages. When appropriate, generic names are indicated. Generic names with * indicate the presence of Fc domain mutations in the clinical product that are not found in the experimental versions used in this paper. Class indicates the Barnes RBD classification (13): class I antibodies bind to the ACE2 binding site when RBD is in the up position; class II bind to the ACE2 binding site when RBD is in the up or down position; class III bind outside the ACE2 binding site when RBD is in the up or down position; and class IV bind outside of the ACE2 binding site when RBD is in the up position. Neutralization in pM is shown. Ranges are indicated with light blue (>67,000 pM), yellow (>10,000 to ≤67,000 pM), orange (>1,000 to ≤10,000 pM), red (>100 to ≤1,000 pM), maroon (>10 to ≤100 pM), and purple (≤10 pM).

A Cross-over dual variable immunoglobulin antibody designs



B Neutralization of SARS-CoV-2 by multispecific antibody candidates

		Omicron Sublineages																pM
		D614G		Beta		Delta		Omicron		Omicron Sublineages								
		IC ₅₀	IC ₉₀	B.1.351		B.1.617.2		BA.1		BA.1.1		BA.2		BA.2.12.1		BA.4/5		
Bispecific and Trivalent	182.1/182.1-61.1	9.1	28.6	31.6	92.9	12.2	31.5	>67,000	>67,000	5920	>67,000	61.0	150	239	689	9697	25350	<div style="background-color: purple; width: 10px; height: 10px; margin-bottom: 2px;"></div> <10 <div style="background-color: maroon; width: 10px; height: 10px; margin-bottom: 2px;"></div> 10-100 <div style="background-color: red; width: 10px; height: 10px; margin-bottom: 2px;"></div> 100-1000 <div style="background-color: orange; width: 10px; height: 10px; margin-bottom: 2px;"></div> 1000-10,000 <div style="background-color: yellow; width: 10px; height: 10px; margin-bottom: 2px;"></div> 10,000-67,000 <div style="background-color: lightblue; width: 10px; height: 10px; margin-bottom: 2px;"></div> >67,000
	182.1/61.1-182.1	22.9	64.0	42.6	113	14.0	43.7	926	7100	294	3053	37.6	85.7	28.2	111	1843	5886	
	61.1/182.1-182.1	75.6	141	158	269	91.1	182	>67,000	>67,000	>67,000	>67,000	112	243	446	683	2552	6118	
	61.1/61.1-182.1	62.0	118	58.6	127	132	246	>67,000	>67,000	>67,000	>67,000	67.7	117	69.8	289	97.3	235	
	61.1/182.1-61.1	26.2	58.3	62.6	137	58.0	122	>67,000	>67,000	27200	>67,000	41.5	96.2	50.7	128	42.7	201	
Trispecific and Trivalent	46.1/61.1-182.1	105	170	269	434	73.2	172	715	2021	841	2221	33.4	83.6	268	638	7735	22043	
	46.1/182.1-61.1	48.5	117	59.8	100.0	237	873	626	3494	804	3293	59.5	125	705	2263	14796	37060	
	61.1/46.1-182.1	30.0	82.6	65.2	127	213	417	175	518	274	500	26.2	42.3	47.9	118	1053	1940	
	61.1/182.1-46.1	80.5	179	217	283	364	587	7754	19729	4778	22779	44.8	117	273	737	1450	4796	







Figure 2. Selection of broadly reactive and potent SARS-CoV-2 monoclonal antibodies

A. Cross-over dual variable (CODV) immunoglobulin antibody designs utilizing variable fragments (Fv) from B1-182.1 (Fv182.1, green), A19-46.1 (Fv46.1, blue) and A19-61.1 (Fv61.1, red). Fc regions contain “knob and hole” feature to increase yield and correct association of heavy chains. Five bispecific trivalent molecules (182.1/182.1-61.1, 182.1/61.1-182.1, 61.1/182.1-182.1, 61.1/61.1-182.1, 61.1/182.1-61.1) and four trispecific trivalent molecules (46.1/61.1-182.1, 46.1/182.1-61.1, 61.1/46.1-182.1, 61.1/182.1-46.1) were designed.

B. Neutralization of candidate multispecific antibodies against D614G and the indicated SARS-CoV-2 variants, including Beta (B.1.351), Delta (B.1.617.2), Omicron (B.1.1.529 or BA.1) and Omicron sub-lineages. Neutralization in pM is shown. Ranges are indicated with light blue (>67,000 pM), yellow (>10,000 to ≤67,000 pM), orange (>1,000 to ≤10,000 pM), red (>100 to ≤1,000 pM), maroon (>10 to ≤100 pM), and purple (≤10 pM).

A

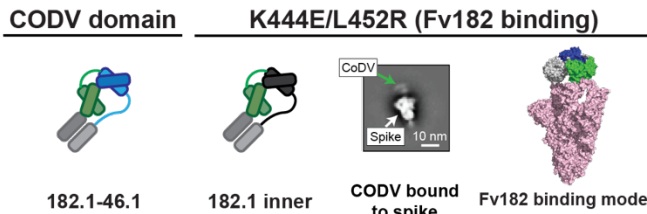
Fv isolating spike mutations

Spike mutations	K444E/L452R	K444E/F486S
Binding allowed	 Fv182	 Fv46
Binding not allowed	 Fv61  Fv46	 Fv61  Fv182

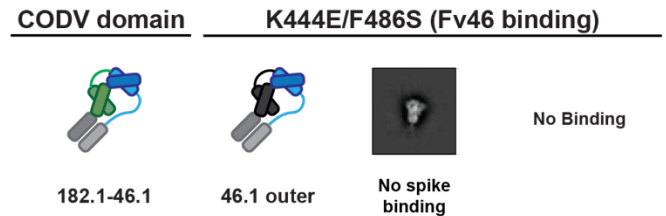
Binding of Fv182

Binding of Fv46

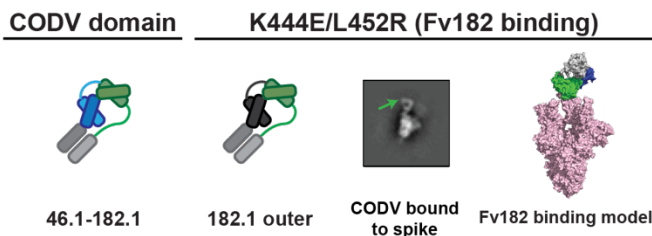
B



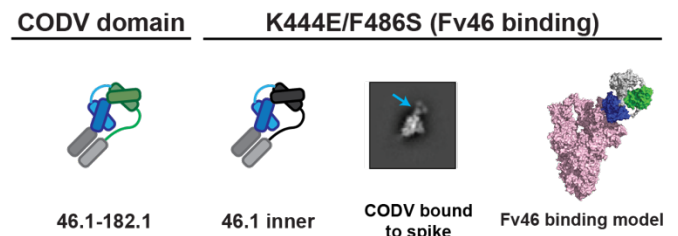
D



C



E



F

46.1-182.1 CODV aggregates Omicron spike proteins

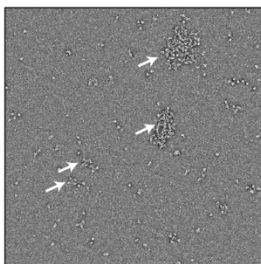


Figure 3. Identification of potential binding modes of CODV to SARS-CoV-2 spike by negative stain-electron microscopy

A. Combination of RBD mutations on the SARS-CoV-2 spike designed to distinguish different binding modes of CODV. Mutations were made in spike in the spike trimer. The domains are colored green, blue, red and gray for Fv182.1, Fv46.1, Fv61.1 and constant domain, respectively.

B-E. Evaluation of CODV Fv182 (B and C) binding to K444E/L452R or CODV Fv46 (D and E) binding to K444E/F486S. Shown at left in each panel is a schematic of the CODV domain being evaluated in the panel. The center-left subpanel indicates the Fv and position being evaluated (i.e., inner or outer). For clarity, the Fv domain that is not able to bind to the mutant is colored black in the subpanels. The center-right subpanel shows the negative stain electron micrograph class averages. Fv182 are indicated with a green arrow and Fv46 with a blue arrow. The white scale bar represents 10 nm in panel C and applies to each micrograph. The rightmost subpanel is a representative model of the binding mode observed in the micrograph. Panels B and C show that irrespective of position, both 182.1-46.1 and 46.1-182.1 are able to bind to spike protein that only allows binding by the Fv182. Panel D, shows that 182.1-46.1 (46.1 outer) is unable to bind spike protein that only allows binding by the Fv46.1. Panel E, shows that 46.1-182.1 (46.1 inner) is able to bind spike that only allows binding by Fv46.

F. CODV 46.1-182.1 induced aggregation of the Omicron spike. Large clusters of aggregation were observed in the negative stain EM field, suggesting the CODV 46.1-182.1 can efficiently promote inter-spike crosslinking.

rcVSV SARS-CoV-2 escape mitigation by most potent and broad trisppecific CoDV antibody

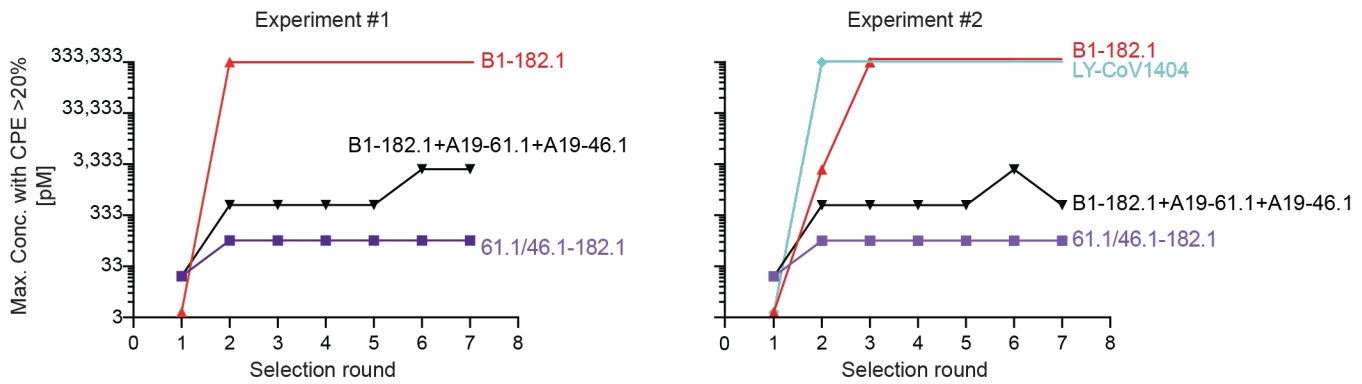


Figure 4. Mitigation of rcVSV escape by 61.1/46.1-182.1 and an antibody cocktail

Replication competent VSV (rcVSV) bearing SARS-CoV-2 WA-1 spike protein was incubated with the indicated antibodies at 5-fold increasing concentrations (34×10^{-3} to 333,333 pM) and added to Vero cells. The appearance of viral growth, as indicated by the presence of >20% CPE, was determined after 3 days and supernatant from the highest antibody concentration with viral growth was passed forward into a new selection round under the same conditions. Once viral growth appeared at 333,333 pM, the antibody was considered fully escaped and supernatant was no longer passed forward. Data is graphed as the highest concentration of antibody at which viral growth was noted in each selection round. Each graph represents an independent experiment.